Novel Pyrolytic Carbon Membranes Containing Silica: Preparation and Characterization

Ho Bum Park, In Young Suh, and Young Moo Lee*

National Research Laboratory for Membrane, School of Chemical Engineering, College of Engineering, Hanyang University, Seoul 133-791, Korea

Received February 19, 2002. Revised Manuscript Received May 7, 2002

A new class of pyrolytic carbon membranes containing silica (C−SiO_2) has been prepared by the pyrolysis of copolyimides consisting of two phases and characterized. To control micropores in the C−SiO_2 membrane, the polyimide copolymer precursors were synthesized via two building blocks that consisted of a carbon-rich phase and a silicon-rich phase. The carbon-rich block consisted of pyromellitic dianhydride and oxydianiline, and the silicon-rich block was oligomeric organosiloxane. These C−SiO_2 membranes were characterized by FT-IR spectroscopy, X-ray diffraction, ESCA, FE-SEM, AFM, and TEM. These analyses revealed that the C−SiO_2 membranes have an asymmetric structure in which the top surface consists of a SiO_2-rich phase in a continuous carbon matrix and the bottom surface is mainly a carbon-rich phase. In a molecular probe study using small molecules (He, O_2, N_2, and CO_2) having sizes from 2.6 to 3.64 Å, the C−SiO_2 membranes exhibited an outstanding molecular sieving capability, together with a high gas permeability. Furthermore, the gas permeation behavior of the C−SiO_2 membrane was very similar to that of the precursor, because the initial morphology of the precursor was well-kept by the use of thermostable components (carbon and silicon) in all blocks after the pyrolysis. The present study provides important information, namely, that the main geometry of the carbon precursor determines the micropore structure and the separation capability of the final pyrolytic carbon membranes.

Introduction

Membrane-based separation science and technology has seen a great upswing in the past few decades, especially in the field of gas separation. Commercial markets for gas separation have made eye-opening progress, in that the performance of membrane materials has improved, exceeding the existing upper bounds[1] for separating gas pairs such as H_2/N_2, He/N_2, O_2/N_2, and CO_2/N_2. In particular, inorganic membranes such as zeolites,[2] sol−gels,[3] and molecular sieving carbon or nanoporous carbon[4] offer significant potential advantages over conventional polymeric membranes. A significant advantage of the inorganic membranes is that they can perform the separation of small molecules under harsh conditions such as elevated temperature and pressure. Simultaneously, to achieve a desirable and practicable flux and selectivity, the microporous inorganic membranes need to have a molecular sieving capability rendered by micropores with dimensions near the sizes of the permeating gas molecules.

Molecular sieving carbons (MSCs) are commonly granular, powdery, or fibrous materials that are expected to be utilized as adsorbents for pressure swing adsorption (PSA), an important gas separation process, and/or as shape-selective catalyst supports. Furthermore, MSCs have been prepared in film-type form (membrane-type) for the past two decades. Since Koresh and Soffer[5] reported the preparation of a carbon membrane in 1983, a variety of carbon membranes have obtained from poly(furfuryl alcohol),[6] phenolic resin,[7,8] polyimides,[9−16] and poly(vinylidene chloride) acrylate terpolymer.[17]

In the preparation of carbon membranes, effective control of the micropores is a crucial factor. It has been demonstrated that, in carbon membranes, such microporosity can be created by channeling molecular debris through a thermosetting polymer matrix during the controlled pyrolysis of synthetic and natural hydrocarbon precursors. An early advance in the development

* To whom correspondence should be addressed. Tel.: +82-2-2291-9683. Fax: +82-2-2291-5982. E-mail: ymlee@hanyang.ac.kr.

(1) Robeson, L. M. *J. Membr. Sci.* **1991**, *62*, 165.
(2) Boudreau, L. C.; Kuck, J. A.; Tsapatsis, M. *J. Membr. Sci.* **1999**, *152*, 41.
(3) Nair, B. N. *J. Membr. Sci.* **1997**, *135*, 237.
(4) Shiflett, M. B.; Foley, H. C. *Science* **1999**, *285*, 1902.
(5) Koresh, J.; Soffer, A. *Sep. Sci. Technol.* **1983**, *18*, 723.
(6) Cheng, Y. D.; Yang, R. T. *Ind. Eng. Chem. Res.* **1994**, *33*, 3146.
(7) Wang, S.; Zeng, M.; Wang, Z. *Sep. Sci. Technol.* **1996**, *31*, 2299.
(8) Katsaros, F. K.; Steriotis, T.; Stubos, A. K.; Mitropoulos, A.; Kanellopoulos, N.; Tennison, S. *Microporous Mater.* **1997**, *8*, 171.
(9) Hatori, H.; Yamada, Y.; Shiraishi, M.; Nakata, H.; Yoshitomi, S. *Carbon* **1992**, *30*, 305.
(10) Jones, C. W.; Koros, W. J. *Carbon* **1994**, *32*, 1419.
(11) Suda, H.; Haraya, K. *J. Chem. Soc., Chem. Commun.* **1995**, 1179.
(12) Hayashi, J.; Yamamoto, M.; Kusakabe, K.; Morooka, S. *Ind. Eng. Chem. Res.* **1995**, *34*, 4364.
(13) Hayashi, J.; Mizuta, H.; Yamamoto, M.; Kusakabe, K.; Morooka, S. *J. Membr. Sci.* **1997**, *124*, 243.
(14) Hayashi, J.; Yamamoto, M.; Kusakabe, K.; Morooka, S. *Ind. Eng. Chem. Res.* **1997**, *36*, 2134.
(15) Kusuki, Y.; Shimazaki, N.; Tanihara, N.; Nakanishi, S.; Yoshinaga, T. *J. Membr. Sci.* **1997**, *134*, 245.
(16) Fuertes, A. B.; Centeno, T. A. *J. Membr. Sci.* **1998**, *144*, 105.
(17) Rao, M. B.; Sicar, S. J. *J. Membr. Sci.* **1996**, *110*, 109.

10.1021/cm020216v CCC: $22.00
Published on Web 06/25/2002

of carbon membranes for gas separation was the finding that the pyrolysis conditions such as temperature, heating protocol, and heating atmosphere have a strong influence on the final membrane structures and properties.[18]

Up to now, studies on carbon membrane have been mostly considered only a few criteria such as the pyrolysis conditions and the type of precursors. Indeed, to effectively control the molecular size and shape-selectivity of the micropores in carbon membranes, the microstructures of the precursors should first be understood for the preparation of high-performance carbon membranes.

Therefore, central to the present study was the aim of finding a new form of template carbonization using self-organized polymeric nanostructure materials (SOPNMs) such as block copolymers consisting of two thermally stable blocks, only inducing the difference of carbon density at the nanoscale. Although carbon itself is perhaps the most thermochemically stable material, it is very susceptible to oxidation, which is an obvious drawback in the efficient and reproducible fabrication of carbon membranes. Moreover, the addition of silicon and/or silicon compounds seems to be a natural choice for the next generation of membrane materials. In particular, carbon and silica play an important role in material science because of their relevance in the academic field and in practical applications. Although the chemical combination of these two materials has been reported in several papers,[19−21] most of the methods used involved the pyrolysis and selective removal of one phase followed by hybridization of polymer and silica sol, resulting in the formation of large mesopores that are not suitable for gas separation.

In the present study, we report a new approach to the preparation of carbon membranes containing silica through the inert pyrolysis of a polymer containing carbon-rich (aromatic microdomain) and silicon-rich (siloxane phase) phases and an examination of the microstructure of the final products. To achieve these objectives, we used imide−siloxane block copolymer (PIS) as a precursor for the present carbon membrane. The rationales for the choice of PIS are as follows: (i) The microstructure of PIS is typically composed of rigid and flexible blocks whose phases give rise to microphase structures. (ii) Two blocks are expected to conserve the initial skeleton and structural characteristics of each domain after heat treatment because two blocks are thermally stable. (iii) Finally, imide blocks are expected to be transformed into a carbon-rich domain (leading to high selectivity) while siloxane blocks are transformed into a carbon-lean phase (resulting in high permeability).

Experimental Section

Materials. Pyromellitic dianhydride (PMDA) and 4,4′-oxydianiline (ODA) were obtained from Tokyo Kasei Co., Inc., Tokyo, Japan, and used without further purification. α,ω-Aminopropyl poly(dimethyl siloxane) (PDMS) was kindly donated by Shinetsu Co., Inc., Tokyo, Japan, and used after being dried in a vacuum oven at 90 °C. Table 1 shows detailed information about the PDMS used in this study. *N*-Methylpyrrolidinone (NMP) and tetrahydrofuran (THF) were obtained from Aldrich Chemical Co., Milwaukee, WI, and dried over 5-Å molecular sieves overnight.

Table 1. Characteristics of Aminopropyl-Terminated Poly(dimethyl siloxane) Oligomers Used in This Study

sample	M_n (g/mol)[a]	n[b]	T_g (°C)[c]
PDMS	900	10	−122

[a] Determined by GPC. [b] Average number of siloxane repeat units in the oligomers. [c] Determined by DSC with a heating rate of 5 °C/min.

Table 2. Sample Designations and Compositions of PISs

sample code	PMDA (mmol)	ODA (mmol)	PDMS (mmol)	volume fraction of siloxane moiety[a]
PIS I	10	9.8	0.2	0.06
PIS II	10	9.0	1.0	0.27
PIS III	10	8.0	2.0	0.46

[a] Calculated by the group contribution method.

Precursor Synthesis. Imide−siloxane block copolymers (PISs) as precursors were synthesized by a two-step polymerization. The chemical composition of the PISs used in this study is summarized in Table 2. Powders of PMDA (10 mmol) were added dropwise to each of three THF solutions of PDMS (0.2, 1.0, and 2.0 mmol) under a nitrogen atmosphere, and then the mixtures were stirred for 1 h. The reaction mixtures were added dropwise to NMP solutions of ODA (9.8, 9.0, and 8.0 mmol). The resulting solutions were stirred at room temperature for 6 h. Homogeneous yellowish siloxane-containing poly(amic acid) (PAA) solutions were then obtained. The solid concentration of PAA was kept at about 10 wt %. The PAA solutions were cast onto a glass plate and then thermally imidized at 100 °C for 1 h, 200 °C for 1 h, 300 °C for 1 h, and 350 °C for 1 h under a vacuum so as to produce strong, flexible, and dense 15−30-μm films. These PIS films were stored until use in a desiccator containing dry silica gel to avoid the influence of humidity.

Pyrolysis Method. Generally, carbon membranes can be prepared by the pyrolysis of suitable polymeric precursors. The carbon membranes obtained in this work were prepared by the pyrolysis of imide−siloxane copolymers with different compositions. Before each pyrolysis trial, the free-standing PIS films were rinsed with deionized water and stored at 120 °C under a vacuum oven until any residual solvent and dust was completely eliminated. After these pretreatments, the PIS films were then pyrolyzed in a muffle furnace equipped with an automatic temperature controller.

The PIS films were pyrolyzed under an Ar flow [<150 cm^3 (STP)/min] in a quartz tube furnace supported on an alumina holder plate. The Ar flow was precisely controlled by a mass flow controller (MKS Instruments, MASS-FLO, Andover, MA). A 4.5-cm-i.d., 70-cm-long quartz tube with a glass end cap was used for the pyrolysis in a muffle furnace equipped with four heating elements to minimize the axial and radial temperature gradients. The length of the effective heating zone was 30 cm, and the maximum heating temperature was 1500 °C.

A pyrolysis protocol was followed precisely to obtain reproducible gas separation properties of the final carbon membranes. The pyrolysis protocol used in this work was determined by the results of thermal gravimetric analysis coupled with mass spectroscopy (TGA-MS). Figure 1 shows the temperature protocol used for the pyrolysis of the precursor films. Prior to heating the furnace, the precursor films were kept for 1 h under an inert purge to stabilize the atmosphere and to remove any humidity in a quartz tube.

The heating rate used in the initial stage was 10 °C/min from room temperature to 400 °C. The heating rate was slowed to 3 °C/min until the temperature reached 600 °C. Then, the PIS films were kept at 600 °C for 2 h (denoted PIS-600). From

(18) Suda, H.; Haraya, K. *J. Phys. Chem. B* **1997**, *101*, 3988.
(19) Rodriguez-Mirasol, J.; Cordero, T.; Radovic, L. R.; Rodriguez, J. J. *Chem. Mater.* **1998**, *10*, 550.
(20) Kyotani, T.; Nagai, T.; Inoue, S.; Tomita, A. *Chem. Mater.* **1997**, *9*, 609.
(21) Müller, H.; Rehak, P.; Jäger, C.; Hartmann, J.; Meyer, N.; Spange, S. *Adv. Mater.* **2000**, *12*, 1671.

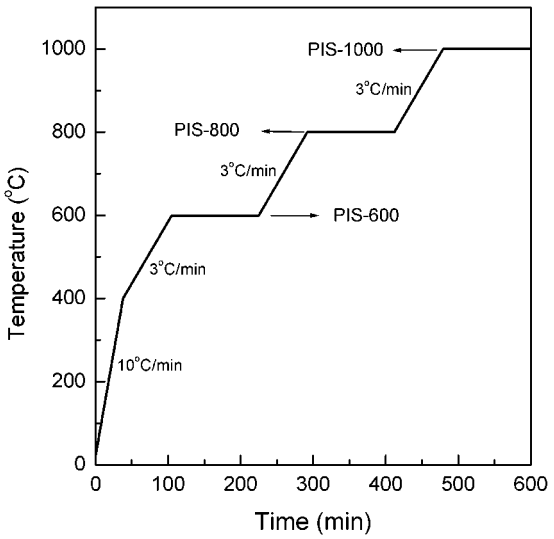

Figure 1. Protocols for pyrolysis of precursors.

600 °C, the heating rate was again ramped to 3 °C/min up to 800 °C. The pyrolyzed PIS films were held at 800 °C for 2 h (denoted PIS-800). Finally, from 800 °C, the heating rate was increased to 3 °C/min until the temperature reached 1000 °C, and the resultant PIS films were held at this temperature for 2 h (denoted PIS-1000). The furnace was allowed to cool slowly to room temperature. The final pyrolytic carbon membranes were taken from the quartz tube and then stored in a desiccator containing dry silica gel to minimize the effects of humidity.

Characterization Methods. The pyrolytic carbon membranes generated from the imide−siloxane copolymers were characterized by the following analysis methods.

1. Fourier Transform Infrared (FTIR) Spectroscopy. The FTIR spectra of the PIS and the pyrolytic carbon membranes were measured by a Nicolet Magna IR 860 instrument (Thermo Nicolet, Madison, WI) in the range of 4000−500 cm^{-1}.

2. Thermal Gravimetric Analysis−Mass Spectroscopy (TGA−MS). TGA was carried out in flowing Ar by use of TGA2050 thermogravimetric analyzer (TA Instruments, New Castle, DE). The amounts of CO, CO_2, H_2, N_2, and CH_4 evolved during pyrolysis were simultaneously determined by QMG 422 high-performance quadrupole mass spectrometer (Balzers Instruments, Liechtenstein). The PIS films were annealed at 400 °C in the TGA apparatus before each analysis to avoid the influence of residual solvent or humidity.

3. Solid-State ^{29}Si Nuclear Magnetic Resonance (^{29}Si NMR) Spectroscopy. Solid-state ^{29}Si NMR spectra of the pyrolytic carbon membranes were measured using a Varian model NMR 1000 spectrometer (Varian Inc., Palo Alto, CA) to observe the change of the siloxane domain in the PIS samples.

4. Wide-Angle X-ray Diffraction (WAXD). An X-ray diffractometer (Rigaku Denki model RAD-C, Rigaku, Tokyo, Japan) was used to evaluate the *d* spacing of the pyrolytic carbon membranes after the pyrolysis.

5. Elemental Analysis (EA). An EA 1110 automatic elemental analyzer (CE Elantech, Inc., Lakewood, NJ) was used to compare the atomic contents (C%, H%, O%, N%) of the PIS films before and after pyrolysis.

6. Transmission Electron Microscopy (TEM). TEM images were recorded using a JEOL JSF-2000FX transmission electron microscope (JEOL, Inc., Kyoto, Japan) at 200 kV to observe the microstructure of the pyrolytic carbon membranes. Samples of the carbon membranes for examination by TEM were prepared by gently scraping the surface layers of the carbon membranes onto carbon-coated TEM grids using a flesh razor blade.

7. Field Emission Scanning Microscopy (FE-SEM). The surface area, cross section, and thickness of the pyrolytic carbon membranes were measured with a field emission scanning microscope (JSF 6330F, JEOL, Inc., Kyoto, Japan) at an accelerating voltage of 15 kV. The polished copper mounts were carbon-coated for conductivity to achieve good imaging.

8. Electron Spectroscopy for Chemical Analysis (ESCA). ESCA analysis was carried out in a Multilab ESCA 3000 instrument (Thermo VG Scientific, East Grinstead, U.K.) to measure the change in chemical composition on the surface of the carbon membrane.

9. Tapping-Mode Atomic Force Microscopy (TM-AFM). For TM-AFM measurements, a Nanoscope II atomic microscope (Digital Instruments, Santa Barbara, CA) and microfabricated cantilevers or silicon probes (Nanoprobes, Digital Instruments, Santa Barbara, CA) with 125-μm-long cantilevers were used at their fundamental resonance frequencies, which typically varied from 270 to 350 kHz, depending on the cantilever, to observe the topology of the carbon membrane surface.

Molecular Probe Study. Molecular probe studies (gas permeation measurements) were conducted using the high-vacuum time-lag method at a feed pressure of 760 Torr and a feed temperature of 25 °C. Before the gas permeation measurements, both the feed and the permeate sides were thoroughly evacuated to below 10^{-5} Torr. The pressure rise versus time transient of the permeate side equipped with a pressure transducer (MKS Baratron type 146) was recorded and passed to a desktop computer through an RS-232 cable. The linear slope of the pressure rise versus time provides the permeation rates of permanent gases. The permeability coefficient for a permanent gas is determined by multiplying the permeation rate by the membrane thickness and can be expressed by

$$P = \frac{\mathrm{d}p}{\mathrm{d}t}\left(\frac{VT_0L}{p_0T\Delta pA}\right) \qquad (1)$$

where P is the permeability represented in Barrer; dp/dt is the rate of the pressure rise under the steady state; V (cm^3) is the downstream volume; L (cm) is the membrane thickness; Δp (cmHg) is the pressure difference between the two sides; T (K) is the measurement temperature; A (cm^2) is the effective area of the membrane; and p_0 and T_0 are the standard pressure and temperature, respectively. Permselectivity as defined in this study is the ratio of permeability of the selected gases to that of nitrogen.

Results and Discussion

FTIR Spectra. Figure 2 shows the FTIR spectra of a precursor film and the pyrolytic carbon films prepared at final pyrolysis temperatures of 600 and 800 °C. The intensities of the absorption bands for aliphatic or aromatic C−N (1100−1200 cm^{-1}, 1300−1400 cm^{-1}), C═O (∼1700 cm^{-1}, 1200−1300 cm^{-1}), and C−H (600−900 cm^{-1}, 1000−1200 cm^{-1}) were reduced at elevated pyrolysis temperature. When the pyrolysis temperature was increased, the Si−O−Si stretching absorption band at 1080 cm^{-1} became broad and was relatively less reduced than the characteristic band of imide. This indicated that a partial Si−O−Si network or silica phase was formed during the pyrolysis of the organosiloxane phase. Generally, a narrow Si−O−Si stretching can be observed in a hybrid such as polyimide−silica, indicating that the silicon environment in the hybrid material is homogeneous and that there are no SiO_4 clusters.[22] However, the Si−O−Si stretching band tends to be broader if silica content is present. This implies the partial formation of a silica phase in the present carbon matrix.

TGA-MS. The thermal properties of the PIS films were observed by means of a thermal gravimetric

(22) Schrotter, J. C.; Smaihi, M.; Guizard, C. *J. Appl. Polym. Sci.* **1996**, *61*, 2137.

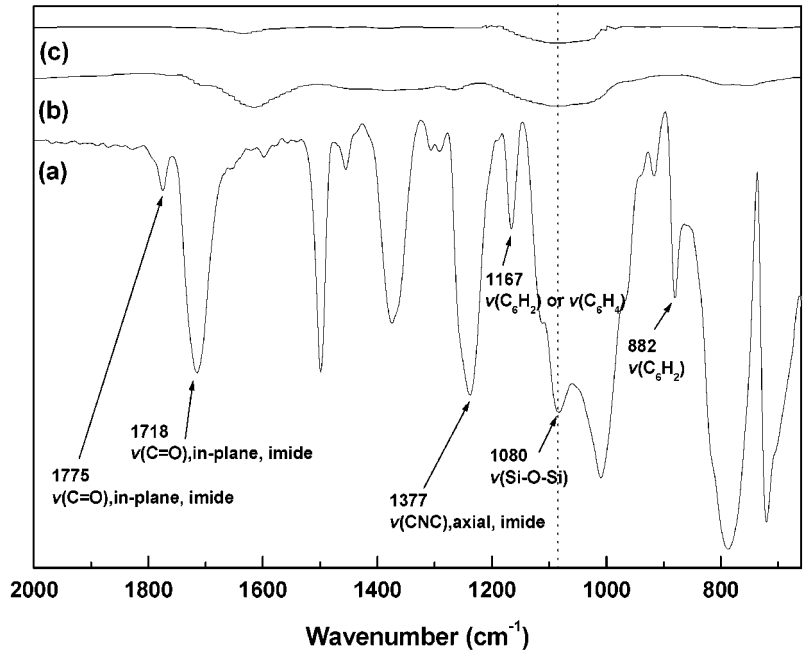

Figure 2. Infrared spectra of (a) original precursor film and pyrolytic films pyrolyzed at (b) 600 and (c) 800 °C.

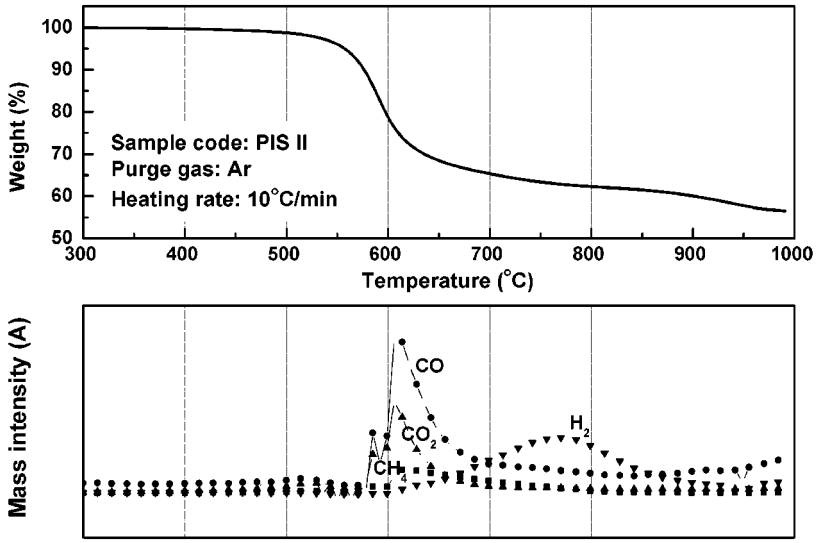

Figure 3. Thermal gravimetric analysis (TGA) curve and mass spectroscopy (MS) results for a PIS film.

analyzer coupled with mass spectroscopy. The weight loss and gas evolution curve was obtained during pyrolysis to 1000 °C at a heating rate of 5 °C/min. The results for PIS II are shown in Figure 3 as a typical example. The TGA and evolution curves are similar to those reported by Inagaki et al.[23] and Hatori et al.[24] In the case of the pyrolysis of Kapton based on PMDA−ODA, imide ring cleavage at 500−600 °C was presumed from the evolution of CO and CO_2. CH_4 evolution due to cleavage of benzene ring was detected around 600−700 °C, and the quantity was very small.[24]

The TGA curve of Kapton−polyimide under Ar purge indicates one main reaction stage (see Figure 4), which is reflected as one peak in the differential thermogravimetric (DTG) curve. Kapton−polyimide is stable up to approximately 600 °C and loses about 50% of its weight at 1000 °C. However, PIS copolyimides start to lose weight at around 500 °C, and their degradation shows two stages of weight loss. As the siloxane content in the PIS matrix increases, the weight loss in the first stage increases, and that in the second stage decreases. Thus, the weight loss in the first stage reflects the decomposition of the siloxane domain, whereas that in the second stage is due to the degradation of oxydianiline. This trend is similar to the thermal degradation of some siloxane-containing polyimides.[25,26] In particular, thermal degradation begins at the aliphatic *n*-propyl segments joining the siloxane segments to the PMDA−ODA-based polyimide. As shown in Figure 4, the overall thermal stability in the first stage decreases as the PDMS content increases because the concentration of

(23) Inagaki, M.; Ishida, T.; Yabe, K.; Hishiyama, Y. *Tanso* **1992**, 244.
(24) Hatori, H.; Yamada, Y.; Shiraishi, M.; Yoshihara, M.; Kimura, T. *Carbon* **1996**, *34*, 201.
(25) Chang, T. C.; Wu, K. H. *Polym. Degrad. Stab.* **1998**, *60*, 161.
(26) Lee, Y. D.; Luo, C. C.; Lee, H. R. *J. Appl. Polym. Sci.* **1988**, *41*, 877.

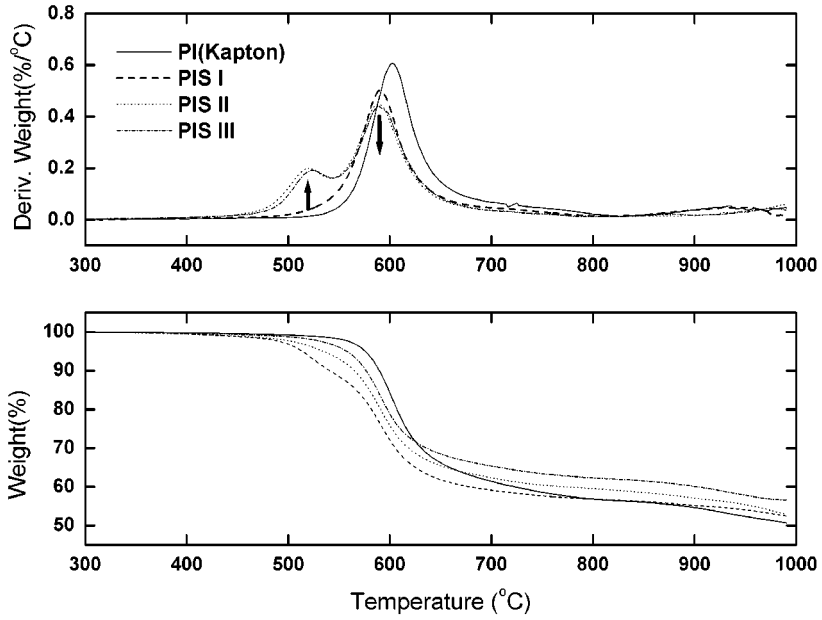

Figure 4. Thermogravimetric analysis (TGA) and differential TGA curves for PIS films.

n-propyl segments in the PIS increases. However, the char yields in the final stage are proportional to the siloxane content because of the partial formation of protective silicon dioxide.

Thus, the thermal decomposition of the imide−siloxane copolymers by pyrolysis proceeds in two steps. The first step of thermal decomposition is the evolution of CO and CO_2 mainly due to breakage at the carbonyl groups in the imide ring and the formation of alkanes by cleavage at the *n*-propyl segments between PDMS and PMDA. The second step, with a small weight loss, involves the evolution of a small amount of H_2. Meanwhile, the random cleavage of $Si-CH_3$ bonds can lead to the formation of methane, with resultant cross-linking of the PDMS segment.

^{29}Si NMR Spectra. Before analyzing the final carbonized structures derived from PIS copolymers, it was presumed that the bulk structure of these pyrolytic carbon membranes consisted of an SiO_2-rich phase having sparse carbon clusters (from the siloxane blocks) within a continuous carbon-rich matrix (from the imide blocks). Thus, to examine the formation of SiO_2 in the pyrolytic carbon matrix, solid-state ^{29}Si cross-polarization magic angle spinning (CP/MAS) NMR spectroscopy was used to evaluate the local environment of the silicon atoms in the bulk state of PIS II pyrolyzed at 600 and 800 °C.

Usually, silicone components are differentiated by the number of oxygen attachments (M = monofunctional, D = difunctional, and Q = silicates, silica, etc.). In the notations D^i and Q^i, *i* refers to the number of Si−O−Si groups bonded to the silicon atom of interest. D^i and Q^i denote species with and without two organic side groups, respectively. In the solid-state ^{29}Si NMR spectra (Figure 5), it was found that D units [$(CH_3)_2SiO$] in the precursor were transformed into Q units of SiO_2 derivatives after thermal treatment. The ^{29}Si NMR spectrum of original PIS II (a) exhibits only one peak at −20.4 ppm, designated as a D^2 structure. This D unit disappears in the spectra of PIS II-600 and PIS II-800. The main signals are observed between −100 and −110 ppm,

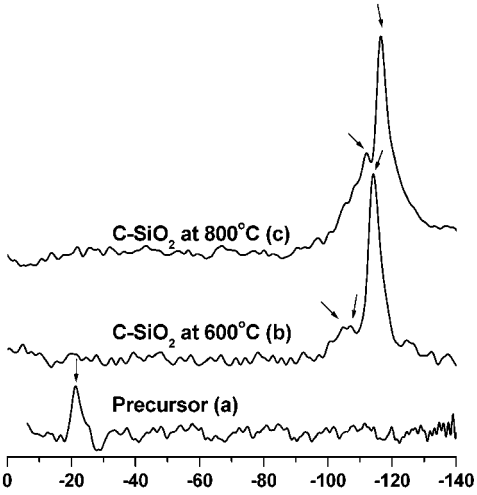

Figure 5. ^{29}Si solid-state NMR spectra of (a) original PIS II, (b) PIS II-600, and (c) PIS II-800.

Table 3. Elemental Analysis of PIS III and Its Pyrolytic Carbon Membranes

	C (%)	Si (%)	O (%)	N (%)	H (%)
PIS III	38.6	3.1	13.4	3.2	41.7
PIS III-600	55.2	5.0	4.6	4.2	31.0
PIS III-800	58.5	6.8	4.8	3.5	26.4
PIS III-1000	69.3	7.2	5.8	3.8	13.9

corresponding, respectively, to Q^3 units [$Si(OR)_1(OSi)_3$ with R = H or CH_3] and Q^4 units [$Si(OSi)_4$]. The presence of Q^i signals in the bulk state verified the formation of $(SiO_2)_x$ within the pyrolytic carbon matrix. However, the intensity of the signal was strongly dependent on both the distance and the number of hydrogen atoms in the environment of the silicon atoms. Therefore, the peak intensity does not accurately represent the population in the sample.

Elemental Analysis. The EA results for the pyrolytic PIS films at each pyrolysis temperature are summarized in Table 3. In the case of PIS III (0.47 volume fraction of the siloxane moiety in the precursor matrix), the yields of carbon and silicon increase with pyrolysis temperature, and the total yield of the two elements

Table 4. *d* spacing of Pyrolytic Powders Calculated from X-ray Diffraction Data

sample	*d* spacing (Å)
PIS I	5.2
PIS I-600	4.2
PIS I-800	4.0
PIS I-1000	3.5
PIS II	5.3
PIS II-600	4.3
PIS II-800	4.2
PIS II-1000	3.6
PIS III	5.7
PIS III-600	4.3
PIS III-800	4.2
PIS III-1000	3.8

reached about 80% of the total composition. The oxygen yield of only 6% implied that −Si−O−Si− groups remained because a large proportion of the oxygen in the imide block (PMDA−ODA) might be released through the evolution of gases such as carbon monoxide and carbon dioxide. Moreover, the bond energy of −Si−O− (545 kJ/mol) is higher than that of −C−O− (340 kJ/mol),[27] and therefore, the remnant of oxygen might result from −Si−O−Si− groups.

X-ray Diffraction. X-ray diffraction is a useful tool for studying the organization of carbon on a molecular level. Although the interatomic distance (1.41 Å) of same-plane carbon atoms cannot be determined by X-ray diffraction, the *d* spacing, a reflection of the interplanar distance, can be measured. By analyzing the X-ray diffraction data, the interlayer spacing can be calculated by applying Bragg's equation to the (100) peak as follows

$$d = \frac{\lambda}{2 \sin \theta} \qquad (2)$$

where *d* is the *d* spacing or interlayer distance.[28] Depending on the extent of carbonization and atomic organization, the *d* spacing for a polymer char can vary from 5 to 3.354 Å.[29] The average interlayer distance for a perfect graphite crystal is 3.354 Å. Given the morphology of glassy carbon from a polymer precursor, the *d* spacing cannot be taken as a true measurement of the interlayer distance, but changes in the *d* spacing can serve as an indicator of the amount of room available for penetrating small molecules.

As shown in Table 4, the *d* spacing of the pyrolytic carbon membranes produced in this study decreased with increasing pyrolysis temperature. Also, the *d* spacings of the samples pyrolyzed at 1000 °C increased slightly from 3.5 to 3.8 Å with increasing siloxane content in the original precursors. At a given pyrolysis temperature, the *d* spacing of the pyrolytic carbon membranes increased with increasing siloxane content in the precursor. This indicates that the siloxane block in the virgin imide−siloxane copolymer affects the interplanar distances of the pyrolytic carbon membranes after pyrolysis.

ESCA. In many phase-separated copolymeric systems, the thermodynamic driving force for minimizing the total free energy of the system, as well as the bulk composition, block length, processing conditions, and block sequence distribution, results in preferential surface segregation of the lower-surface-energy constituent.[30−32] In particular, polysiloxanes are generally used as a surface modifier through blending or copolymerization with other polymers, because of the free rotatability and polarizability of the Si−O bond.[33] Consequently, the −Si−O−Si− chain is able to align itself accordingly, resulting in a rich in-depth distribution of the surface in copolymers and blends. Thus, some of the most interesting and unique features of siloxane-containing copolymers are associated with their surface morphology and the resultant surface properties. Poly(dimethylsiloxane) (PDMS) has extremely low surface tension and surface energies because of its very large molar volume combined with its very low cohesive energy density and high flexibility. For linear PDMS, the surface tension is from 12 to 15 dyn/cm.[33] This is at least 10 dyn/cm lower than the surface tensions of many other polymeric systems. As a result, the air−polymer surfaces of siloxane-containing copolymers as well as their blends with other polymers are substantially enriched in the lower-surface-energy siloxane. To achieve the desired surface modification, only a small amount of siloxane content (1−2 wt %) is usually needed. For these reasons, the PISs used as precursors in this study have an asymmetric morphology consisting of a siloxane-rich top surface and an imide-rich bulk. Thus, we focused on the characteristic properties of the siloxane-based copolymers and assumed a SiO_2-rich top surface in the present carbon membranes after pyrolysis.

To examine this assumption regarding the surface of the present pyrolytic carbon membranes, hydrogen fluoride (HF) acid etching was conducted to remove, most likely, the SiO_2 phase on the surface of the pyrolytic carbon membrane. Here, ESCA was used to reveal the surface composition of the carbon membranes before and after the acid treatment.

Full-scanning ESCA spectra of the carbon films before and after the acid etching were compared as shown in Figure 6a. Signals from four detectable elements (carbon, oxygen, nitrogen, and silicon) were recorded at 284.2 (C_{1s}), 543.1 (O_{1s}), 409.9 (N_{1s}), and 103.6 eV (Si_{2p}). After the acid treatment, the Si_{2p} peak became barely detectable compared to the corresponding peak before the acid treatment, as shown in Figure 6b (high-resolution ESCA spectra of Si_{2p}). Generally, the Si_{2p} spectrum can be fitted with two components in silicon compounds: Si(I) at 101.5 eV and Si(II) at about 103.6 eV. It is well-known that Si(I) and Si(II) can be attributed to PDMS and SiO_2, respectively.[34] We do not observe a Si(I) spectrum corresponding to the existence of dimethylsiloxane after the pyrolysis. These ESCA spectra confirm that the present carbon matrix has a

(27) Brook, M. A. *Silicon in Organic, Organometallic, and Polymer Chemistry*; John Wiley & Sons: New York, 2000; p 30.
(28) Zachariasen, W. H. *Theory of X-ray Diffraction in Crystals*; John Wiley & Sons: New York, 1945; p 85.
(29) Jenkins, G. M.; Kawamura, K. *Polymeric Carbons−Carbon Fibre, Glass, and Char*; Cambridge University Press: New York, 1976; p 60.
(30) Zhao, J.; Rojstaczer, S. R.; Chen, J.; Xu, M.; Gardella, J. A., Jr. *Macromolecules* **1999**, *32*, 455.
(31) Chen, X.; Gardella, J. A., Jr.; Ho, T.; Wynne, K. J. *Macromolecules* **1995**, *28*, 1635.
(32) Li, L.; Chan, C. M.; Weng, L. T. *Macromolecules* **1997**, *30*, 3698.
(33) Yilgör, I.; McGrath, J. E. *Adv. Polym. Sci.* **1988**, *86*, 1.
(34) Feng, J.; Weng, L.-T.; Chan, C.-M.; Xhie, J.; Li, L. *Polymer* **2001**, *42*, 2259.

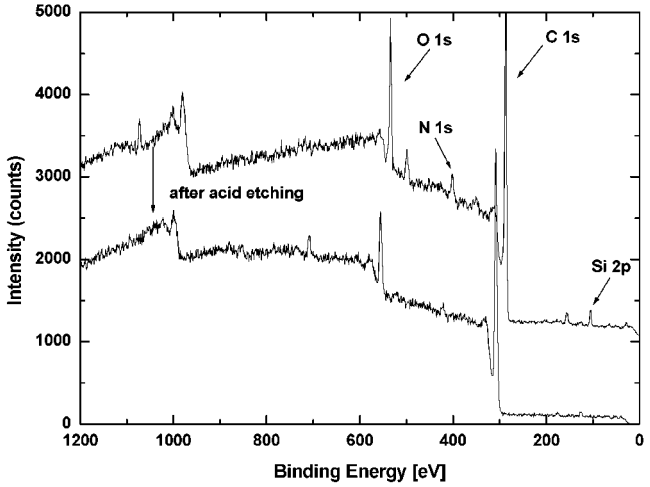

(a)

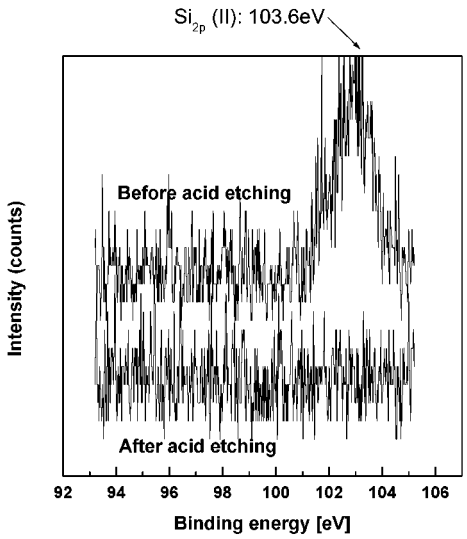

(b)

Figure 6. ESCA spectra of (a) full scan, (b) high-resolution of Si_{2p} before and after HF acid etching.

SiO_2-rich structure on the surface similar to the in-depth structure found in siloxane-containing copolymers.

TM-AFM. TM-AFM (Digital Instruments, Nanoscope II) was used to study the surface morphology of the carbon precursor and carbon membranes before and after HF acid etching. The surface topography of the precursor included hills and valleys because of the difference in solubility of the two domains during solvent evaporation (Figure 7a). Note that the surface topographies of the carbon films before and after acid etching are very different as a result of the removal of the SiO_2-rich phase from the surface, as shown in Figure 7b and c. The surface morphology of the carbon films is rough, indicating selective removal of the plentiful SiO_2 phase from the surface of the carbon film after acid etching. This is in a good agreement with our previous ESCA results. The topmost surface morphology of the carbon membranes after acid etching was similar to that further illustrated by the FE-SEM images.

FE-SEM Images. While observing the surface morphology on both sides of the carbon film after HF treatment at room temperature by FE-SEM, very interesting features were found. The surface of only one side (air−polymer interphase) (Figure 8) of the carbon membrane was observed to contain well-distributed carbon spheres with grains shaped in the form of discrete bright spots. The spheres had a nearly constant size of about 200−220 nm in diameter. A separate energy-dispersive X-ray spectrometry (EDX) analysis (Figure 8a) confirmed that these spheres of carbon grains formed after the removal of the SiO_2-rich surface. The reason the carbon spheres formed on the top surface (air−polymer side) might be related to the surface and bulk morphology of the poly(imide siloxane) precursor. At present, it is speculated that the siloxane-rich phase on the top surface is a continuous phase whereas the imide segments form a dispersed phase. In the bulk state, however, the situation is reversed. Therefore, the carbon spheres appeared on the top surface after HF etching because of the imide blocks dispersed in the siloxane-rich top surface. That is, the present carbon matrix forms an asymmetric structure consisting of a SiO_2-rich surface and a carbon-rich matrix.

The carbon spheres found in the FE-SEM image were observed again by transmission electron microscopy. Figure 9 shows that a considerable improvement in structure occurs and some turbostratic carbon layers appear in the stacking order of the hexagonal carbon layers in the carbon spheres (obtained from PIS II films pyrolyzed at 800 °C after HF treatment). Consequently, the present carbon membranes are called C−SiO_2 membranes, where carbon forms a continuous matrix and SiO_2 is an embedded phase in the bulk state.

TEM Images. Powdery samples of C−SiO_2 membranes for an examination by TEM were prepared by carefully scraping the cross section of the C−SiO_2 membrane onto carbon-coated TEM grids using a sharp razor blade. Notice in Figure 10 that the C−SiO_2 membranes are composed of amorphous and partially turbostratic-like carbon structures and also that they can be divided into carbon-rich (black region, PMDA−ODA) and carbon-poor (white region, PDMS) domains.

Usually, in the case of the carbon membranes prepared by the pyrolysis of organic polymers between 650 and 2200 °C, the carbon structure obtained is known to have a turbostratic structure, in which planar layers of graphite-like microcrystallines are dispersed in a noncrystalline and amorphous carbon. Indeed, the nanometric texture in the cross section of carbon films derived from Kapton−polyimide (PMDA−ODA) by heat treatment changes from turbostratic (650−1000 °C) to turbostratic with flattened pores (2200 °C), partially graphitic (2300 °C), mostly graphitic (2500 °C), and finally graphitic (3000 °C).[35]

TEM images of the C−SiO_2 membranes demonstrated some peculiar features. The change in morphology was found to result from the existence of a SiO_2 phase that might be composed of carbon-poor clusters, that is, clusters with low carbon density. Furthermore, it was somewhat interesting that a concentric circle−layered carbon structure was found during the pyrolysis of an organic polymer containing heterogeneous atom such as silicon or a silica phase at relatively low temperature (600−1000 °C).

(35) Inagaki, M. *New Carbon*; Elsevier: New York, 2000.

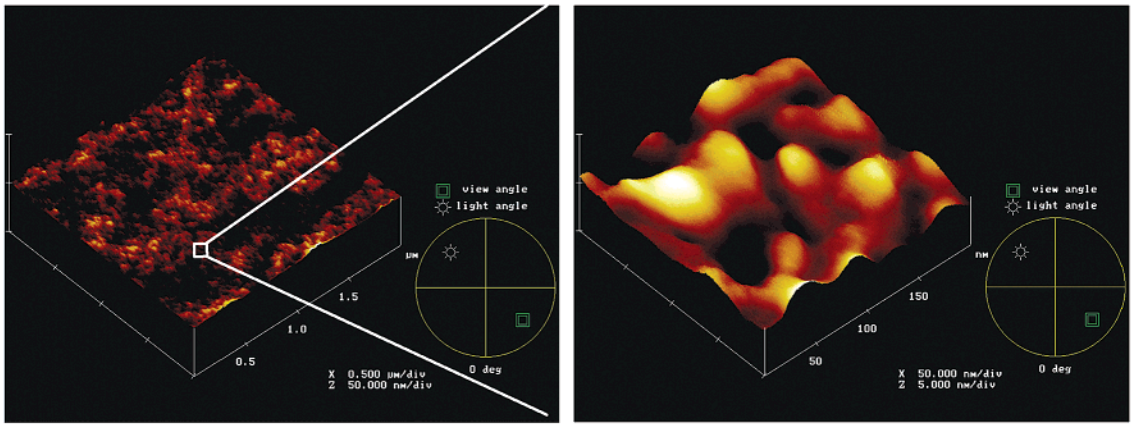

(a)

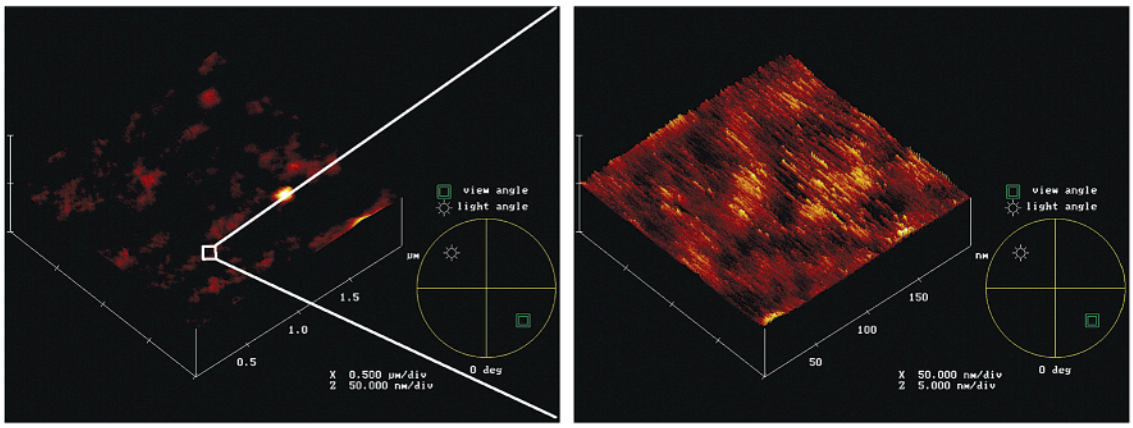

(b)

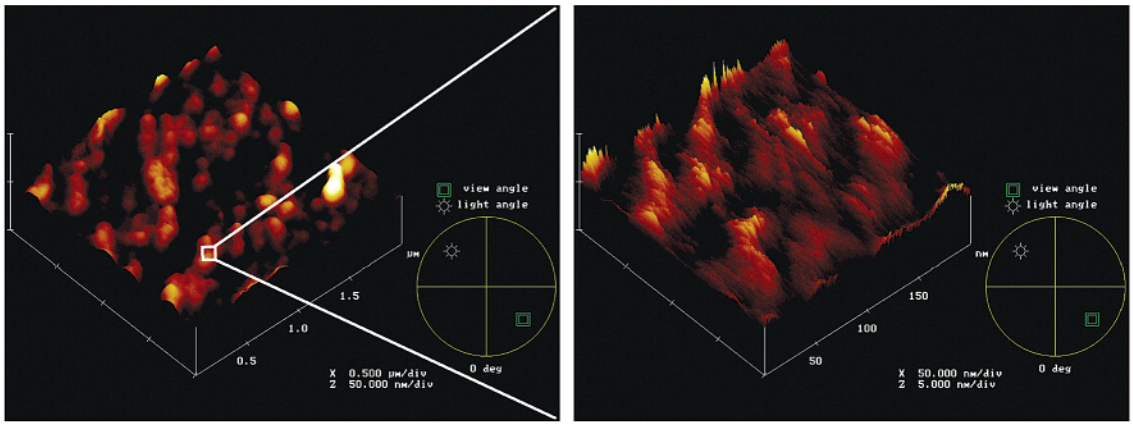

(c)

Figure 7. TM-AFM images of (a) PIS II, and PIS II-800 (b) before and (c) after acid etching.

Molecular Probe Study. To evaluate the molecular sieving capability of the C−SiO_2 membranes, molecular probe studies were carried out to measure pure-component gas permeabilities through the membranes using nitrogen (N_2, 3.64 Å), oxygen (O_2, 3.46 Å), helium (He, 2.60 Å), and carbon dioxide (CO_2, 3.36 Å).

One of the main objectives of this work was to study the changes in properties of a precursor composed of carbon-rich (PMDA−ODA) and silicon-rich (PMDA−PDMS) domains during pyrolysis. The pyrolysis conditions, including the pyrolysis temperature, the heating rate, and the pyrolysis atmosphere, are important factors in determining the microstructure and gas permeation properties of pyrolytic carbon membranes.

In the present work, it was observed that the pyrolysis temperature had a marked influence on the permeation characteristics of the C−SiO_2 membranes produced. Figures 11−13 illustrate the He, O_2, N_2, and CO_2 permeabilities at 25 °C for C−SiO_2 membranes prepared at different pyrolysis temperatures (600, 800, and 1000 °C). The gas permeabilities of the selected gases were shown to be in the order He > CO_2 > O_2 > N_2. Usually,

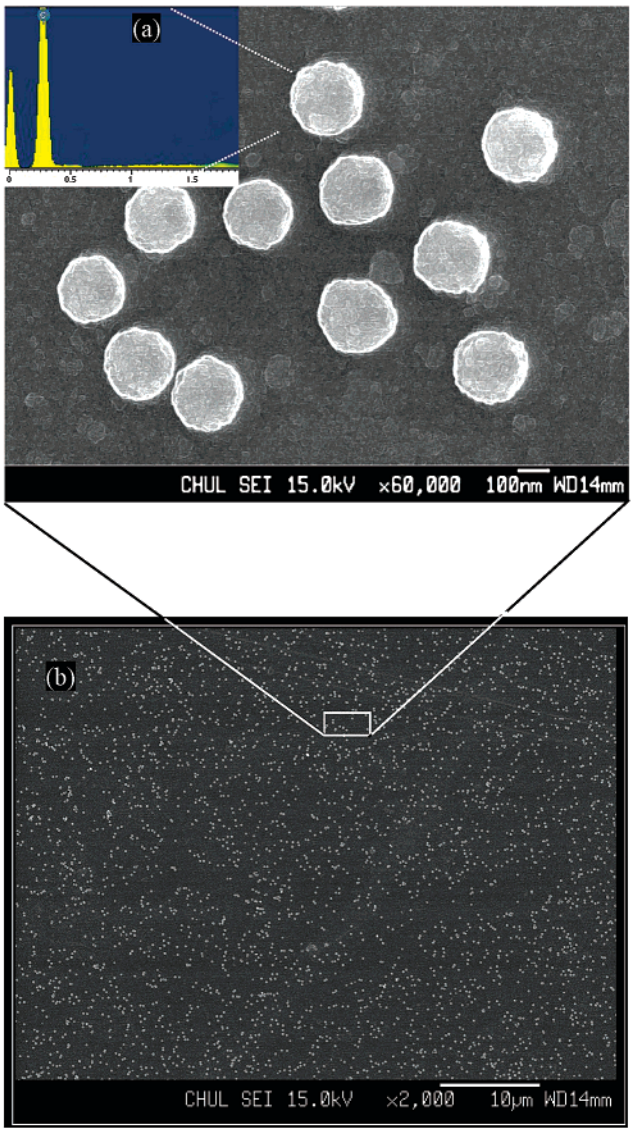

Figure 8. FE-SEM image of top surface (air−polymer interphase) of pyrolytic carbon films after HF acid etching (a) ×60 000 with EDX spectra and (b) ×2000.

the permeabilities of small gases through microporous membranes such as carbon molecular sieves and/or silica membranes are in agreement with the order of the kinetic gas diameters, except in some peculiar cases. That is, the gas transport mechanism through these membranes occurs by a diffusion-dominant mechanism or a size-exclusive mechanism.

All of the gas permeabilities increased with increasing pyrolysis temperature up to 800 °C. As shown in Figures 11−13, the gas permeabilities through the C−SiO_2 membranes reached a maximum value at 800 °C. However, as the pyrolysis temperature increased to 1000 °C, the resulting C−SiO_2 membranes were less permeable than those pyrolyzed below 800 °C. In the case of the C−SiO_2 membrane derived from PIS II, the pyrolysis of the polymeric precursor at 1000 °C led to an oxygen permeability of only 2 Barrer in comparison with 68 Barrer for pyrolysis at 800 °C. This behavior was confirmed by nitrogen gas adsorption experiments [BET (Brunauer−Emmett−Teller) method], as shown in Figure 14.

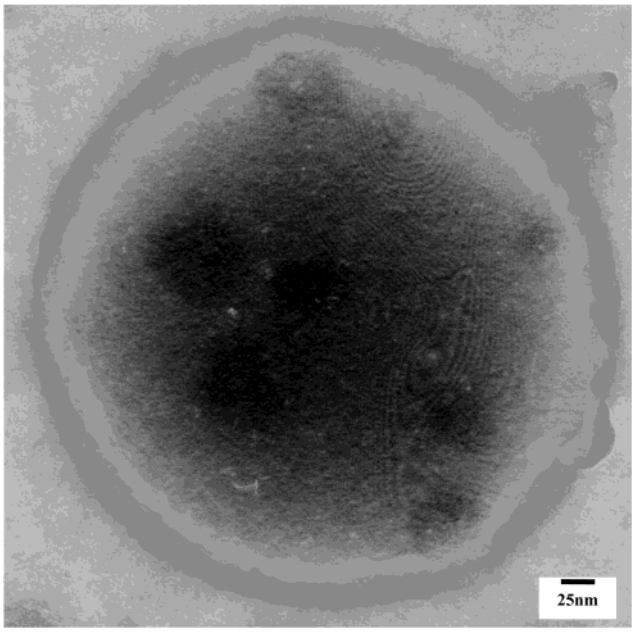

Figure 9. TEM image of carbon sphere appearing in top surface after HF acid etching.

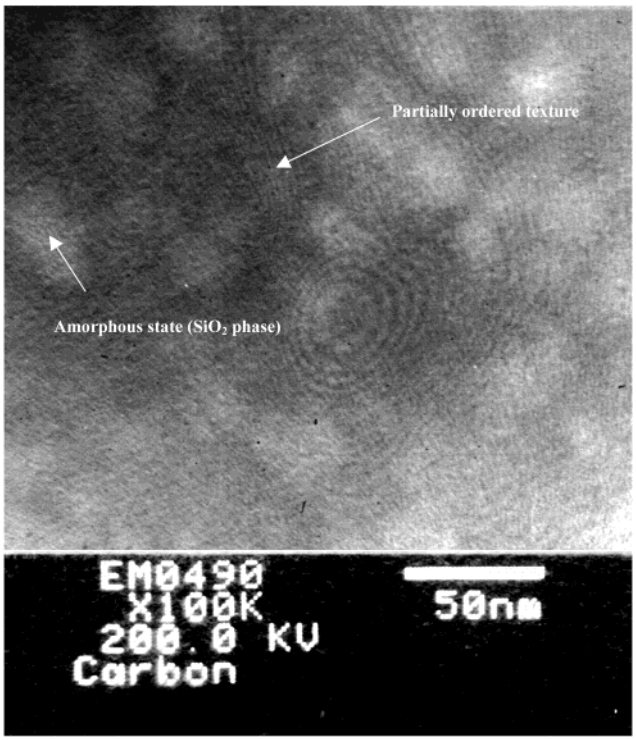

Figure 10. TEM image of C−SiO_2 membrane prepared by pyrolysis at 1000 °C.

The volume of nitrogen absorbed in the C−SiO_2 membrane prepared at 800 °C was greater than those in the C−SiO_2 membranes prepared at 600 and 1000 °C. This indicates the formation of transient open pores in the domain of the SiO_2-rich network at around 800 °C in the continuous carbon matrix. This is in good agreement with the results of the gas permeation experiments. The nitrogen adsorption results for the 600 and 1000 °C pyrolyzed C−SiO_2 membranes exhibit the characteristics of Langmuir (or type I) isotherms, which implies that they are microporous materials. The iso-

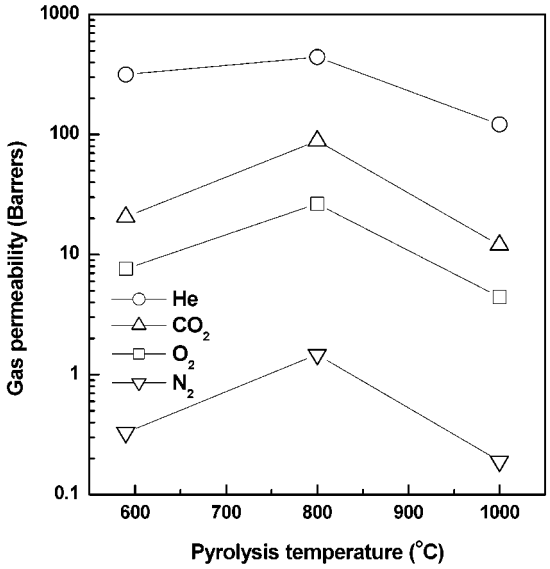

Figure 11. Gas permeabilities as a function of pyrolysis temperature for C−SiO_2 membrane derived from PIS I.

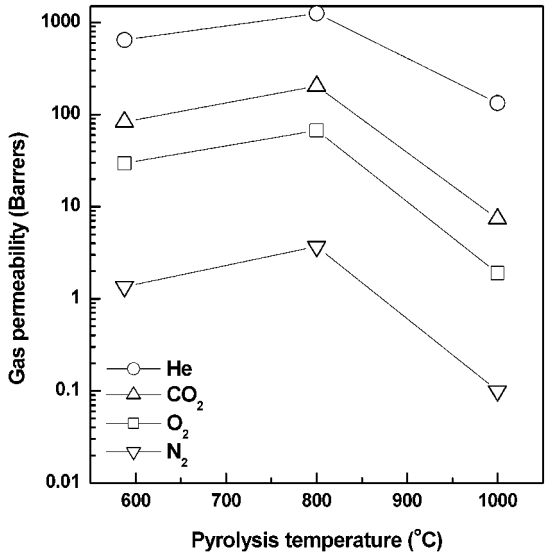

Figure 12. Gas permeabilities as a function of pyrolysis temperature for C−SiO_2 membrane derived from PIS II.

therms of the C−SiO_2 membrane pyrolyzed at 800 °C shows the adsorption characteristics of type IV. The 800 °C isotherm shows that the adsorption undergoes an increase at $P/P_0 > 0.7$ and a hysteresis, which indicates that a number of ink-bottle-like pores are generated at 800 °C. Although pores with diameters of less than 1.7 nm are not measured, Figure 14 demonstrates that the pyrolysis operation both opens and sinters the pores of the C−SiO_2 membranes with pyrolysis temperature.

In the present work, pyrolysis temperatures of around 800 °C represent an optimum from the standpoints of permeation rate and permselectivity. Moreover, this pyrolysis-temperature-dependent gas permeation behavior can be described by the variation in the open porosity of the polysiloxane domain with the pyrolysis temperature. Cordelair and Greil[36] recently reported that polysiloxanes $[RSiO_{1.5}]_n$ with R = CH_3 (PMS) and

(36) Cordelair, J.; Greil, P. *J. Eur. Ceram. Soc.* **2000**, *20*, 1947.

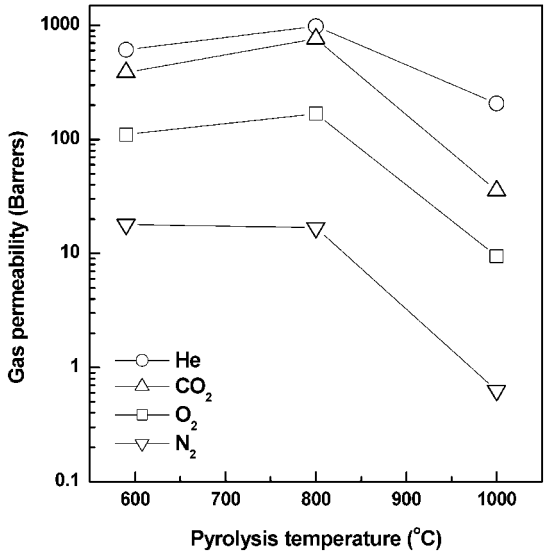

Figure 13. Gas permeabilities as a function of pyrolysis temperature for C−SiO_2 membrane derived from PIS III.

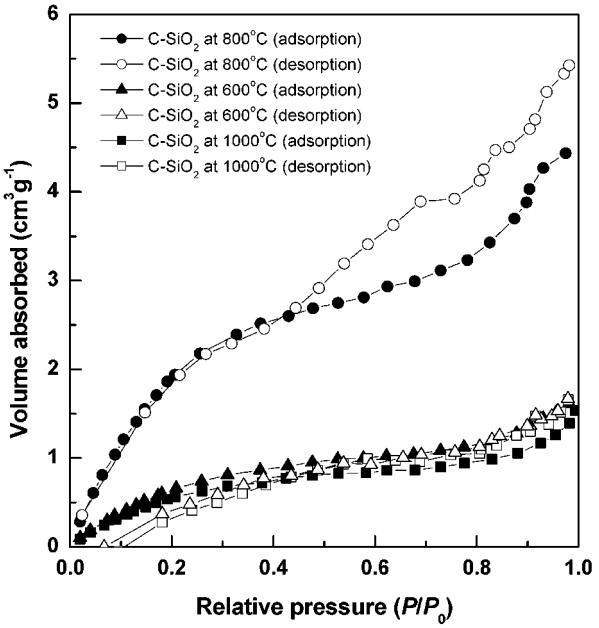

Figure 14. Nitrogen adsorption isotherms for the C−SiO_2 membranes prepared from the PIS II precursor.

C_6H_5 (PPS) were transformed to Si−O−C ceramics of variable composition and structure upon pyrolysis in an inert atmosphere at 500−1500 °C. They used mercury intrusion measurements to confirm the formation of large transient open pores in the temperature range where thermal degradation occurred and revealed that open porosity (volume percent) reached a maximum value at a pyrolysis temperature of 800 °C in the case of the polysiloxane with the methyl group. This result is in a good accordance with the maximum gas permeabilities of C−SiO_2 in the present study, assuming that the gas transport could occur preferentially in the carbon-poor region, i.e., the SiO_2 phase.

The O_2 permeabilities and the selectivities of O_2/N_2 of the C−SiO_2 membrane prepared at 800 °C are represented as a function of initial siloxane content in the precursor matrix in Figure 15. The gas permeabili-

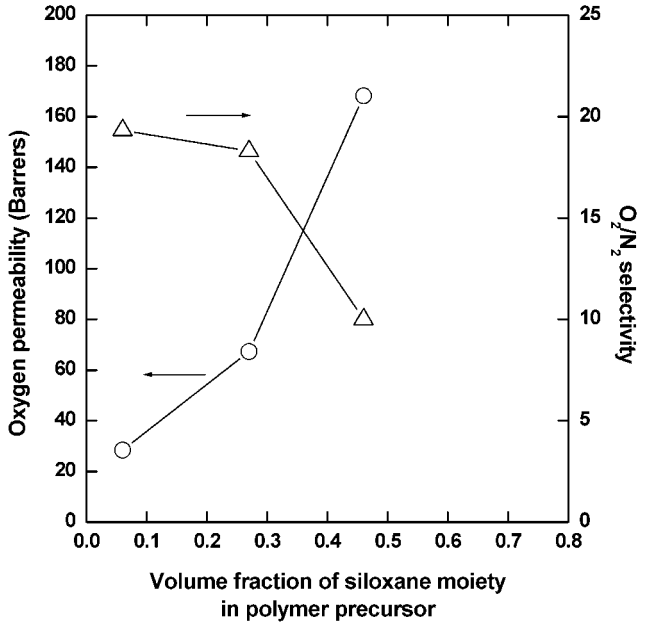

Figure 15. O_2 permeabilities and O_2/N_2 selectivities of C−SiO_2 membranes prepared by pyrolysis at 800 °C as a function of the volume fraction of siloxane in the precursor.

Table 5. Gas Permeation Results for C−SiO_2 Membranes at 25 °C

pre-cursor	pyrolysis temp (°C)	permeability (Barrer)[a]				selectivity to N_2		
		He	O_2	CO_2	N_2	O_2/N_2	CO_2/N_2	He/N_2
PIS I	600	315	7.6	21	0.33	23	62	955
	800	442	27	89	1.47	18.4	61	304
	1000	121	4.5	12	0.19	24	64	643
PIS II	600	1258	30	84	1.35	22.2	62	1033
	800	1393	68	204	3.68	18.5	56	341
	1000	133	2	7.4	0.10	20	74	1330
PIS III	600	610	111	386	18	6.2	21	34
	800	981	168	765	16.8	10	46	58
	1000	207	9.5	36	0.63	15	57	56

[a] 1 Barrer = 10^{-10} cm^3(STP)·cm/cm^2·s·cmHg.

ties and the selectivities to nitrogen of all of the samples are summarized in Table 5. Note that the O_2 permeabilities of the C−SiO_2 membranes tend to increase with increasing volume fraction of the initial siloxane moiety in the original imide−siloxane copolymer matrix but that the O_2/N_2 selectivities decrease from 19 to 10.

It is worth mentioning the gas permeation properties of the polymeric precursor used before pyrolysis, because the microstructure of a polymer is closely related to its gas transport behavior. Our previous works on the gas permeation behavior of precursors reported on the transport behavior of rigid−flexible block copolymer membranes such as poly(amideimide siloxane) and poly(imide siloxane).[37,38] For polyimides into which a siloxane moiety had been introduced, the oxygen permeability increased from 1 to 100 Barrer, but the selectivity of O_2/N_2 selectivity decreased from 10 to 2.5 with an increase in the siloxane content. Interestingly, it was observed that the oxygen permeability dramatically increased at a ∼0.2−0.3 volume fraction of siloxane in the copolymer matrix. The percolation concept, meaning the formation of the effective shortest path around this composition, was introduced and applied to explain this behavior. Indeed, the structure of poly(imide siloxane) could be explained by a two-phase model with a partially mixed interphase. Unlike block copolymers with well-ordered microphase-separated structures, poly(imide siloxane) forms a segmented block copolymer in which the geometric disorder, that is, the random segment size distribution, forces the mixing of the hard (rigid) and soft (flexible) segments. Thus, this randomly ordered two-phase system is very similar to a percolating system in which two components with different characteristics are randomly mixed. Furthermore, a partially mixed interface between the two phases might easily lead to connected phases with the gradual addition of one phase. From these results, it was assumed that the carbonization of these block copolymers with two characteristic domains should lead to changes in the gas permeation properties. Also, the effect of a heterophase such as SiO_2 on the gas separation properties of pyrolytic carbon membranes should be seriously considered.

As shown in Figure 15, the O_2 permeability increased at around 0.3 volume fraction of siloxane in the precursor, indicating that the characteristic skeleton of the two phases might be considerably conserved even after the pyrolysis. Indeed, the rigid imide domain composed of the aromatic backbone and the the flexible siloxane domain performed the roles of "organic molecular sieve" and "percolator", respectively. After the transition from the organic to the inorganic phase by the heat treatment, the imide and siloxane domains were gradually changed into a "carbon-rich" phase with cross-linked voids of amorphous regions and the interlayer spacing of graphite-like or highly ordered microcrystalline carbon and a "SiO_2-rich" phase with sparse carbon clusters.

Figure 16 illustrates a hypothetical model of the major structural transitions occurring during the heat treatment of the different domains, imide and siloxane. During pyrolysis, the imide domain might preferentially change into a carbon-rich domain, building carbon clusters and a carbon network, whereas the siloxane domain might change into a carbon-lean domain with partial carbon clusters. The domains with no graphite-like carbon network provide a broad pathway for the permeant, and simultaneously, the domains with a substantial carbon network contribute to the diffusional selectivity. This model can be verified by the observations of the gas permeation behavior in the membrane before and after pyrolysis. Consequently, this implies that microphase control of the precursor is a key to preparing highly permselective pyrolytic carbon membranes.

The diffusion coefficients and diffusional selectivities of O_2 and N_2 are summarized in Table 6. The diffusional selectivities of C−SiO_2 membranes are usually higher than those of typical polymeric membranes. The high selectivity of the C−SiO_2 membranes is attributed mainly to the increase in diffusional selectivity. Generally, nonporous polymers and molecular sieving matrixes such as carbon molecular sieves and zeolites transport gas molecules by a similar sorption−diffusion mechanism. The permeability of a penetrant through a membrane is measured as a steady-state flux, normal-

(37) Park, H. B.; Ha, S. Y.; Lee, Y. M. *J. Membr. Sci.* **2000**, *177*, 143.
(38) Ha, S. Y.; Park, H. B.; Lee, Y. M. *Macromolecules* **1999**, *32*, 2394.

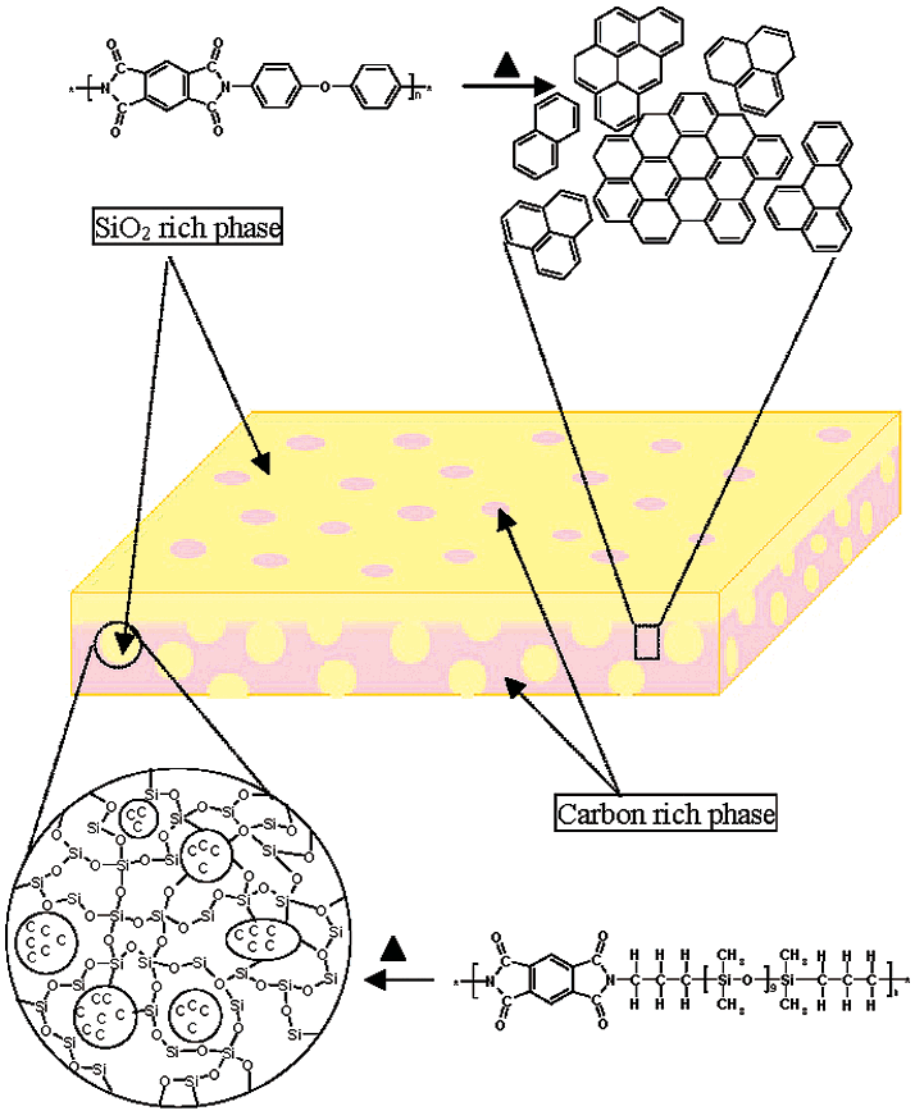

Figure 16. Proposed model of the present C−SiO_2 membrane inferred from bulk and surface analysis and molecular probe studies.

Table 6. O_2 and N_2 Diffusion Coefficients ($cm^2 \cdot s^{-1} \times 10^9$) and Diffusion Selectivities of C−SiO_2 Membranes at 25 °C

precursor		600 °C	800 °C	1000 °C
PIS I	O_2	1.38	5.82	1.09
	N_2	0.14	0.36	0.11
	$D(O_2)/D(N_2)$	10	15.5	9.9
PIS II	O_2	4.55	9.48	0.89
	N_2	0.50	0.65	0.10
	$D(O_2)/D(N_2)$	9.1	14.6	8.9
PIS III	O_2	48.60	10.65	0.62
	N_2	15.00	1.03	0.07
	$D(O_2)/D(N_2)$	3.2	10.3	8.3

ized by the partial pressure difference and the membrane thickness. The permeability of component A can be expressed as the product of a kinetic factor, the diffusion coefficient (D_A), and a thermodynamic factor, the sorption coefficient (S_A)

$$P_A = D_A S_A \tag{3}$$

The ideal permselectivity, $\alpha_{A/B}$, characterizes the overall ability of a membrane to separate penetrants A and B. This is an inherent property of the material and its molecular geometry. The permselectivity can be factored into terms for diffusion selectivity and sorption selectivity as follows

$$\alpha_{A/B} = \frac{P_A}{P_B} = \frac{D_A}{D_B}\frac{S_A}{S_B} \tag{4}$$

Generally, the sorption-selectivity term for the O_2/N_2 pair lies in the range of 1−2 for almost all glassy polymers and in the range of 0.7−2 for molecular sieving materials such as zeolites and carbon molecular sieves. Therefore, as shown in Table 6, it is the diffusion selectivity of the C−SiO_2 membranes in the present study that is responsible for the remarkable differences in their separation properties.

Conclusions

In the present study, we have shown that a novel carbon-implanted SiO_2 (C−SiO_2) can be readily prepared by pyrolyzing a precursor that combines two building blocks with different carbon densities on the nanoscale. The C−SiO_2 membranes prepared by carbonization of the new template form an asymmetric

morphology in which the top surface consists of a SiO_2-rich phase in a continuous carbon matrix and the bottom surface is mainly a carbon-rich phase. A molecular probe study using small penetrant molecules revealed that the $C-SiO_2$ membranes separated small molecules very efficiently by a molecular sieving mechanism. The O_2/N_2 selectivity versus O_2 permeability for the $C-SiO_2$ membranes was, to the best of our knowledge, higher than the values obtained with other gas separation carbon membranes. However, the ideal gas separation factor obtained in single-gas permeation experiments can be different from that obtained in mixed-gas permeation experiments. We will report a comparison of data from single-gas and mixed-gas permeation experiments in the near future.

Acknowledgment. This work was conducted with the support of Korea Institute of Science & Technology Evaluation and Planning (KISTEP) under National Research Laboratory (NRL) Program. H.B.P. and I.Y.S. are grateful to the Brain Korea (BK) 21 Project for fellowships. PDMS samples from Shinetsu Chemical Co., Inc., are greatly appreciated.

CM020216V